Materials Research Bulletin 50 (2014) 12–17

Contents lists available at ScienceDirect

Materials Research Bulletin

journal homepage: www.elsevier.com/locate/matresbu

# Photoluminescence emission at room temperature in zinc oxide nano-columns

L.S.R. Rocha [a], R.C. Deus [a], C.R. Foschini [c], F. Moura [b], F. Gonzalez Garcia [b], A.Z. Simões [a,*]

[a] Universidade Estadual Paulista – Unesp, Faculdade de Engenharia de Guaratinguetá, Av. Dr. Ariberto Pereira da Cunha, 333, Bairro Portal das Colinas, CEP 12516-410 Guaratinguetá, SP, Brazil[1]

[b] Universidade Federal de Itajubá – Unifei, Campus Itabira, Rua São Paulo, 377, Bairro Amazonas, CEP 35900-37 Itabira, MG, Brazil[2]

[c] Universidade Estadual Paulista – Unesp, Instituto de Química, Laboratório Interdisciplinar em Cerâmica (LIEC), Rua Professor Francisco Degni s/n, CEP 14800-90 Araraquara, SP, Brazil[3]

ARTICLE INFO

*Article history:*
Received 11 April 2013
Received in revised form 6 September 2013
Accepted 29 September 2013
Available online 8 October 2013

*Keywords:*
A. Nanostructures
B. Chemical synthesis
C. Electron microscopy
D. Luminescence
D. Crystal structure

ABSTRACT

Hydrothermal microwave method (HTMW) was used to synthesize crystalline zinc oxide (ZnO) nano-columns at the temperature of 120 °C with a soaking time of 8 min. ZnO nano-columns were characterized by using X-ray analyses (XRD), infrared spectroscopy (FT-IR), thermogravimetric analyses (TG-DTA), field emission gun and transmission electron microscopy (FEG-SEM and TEM) and photoluminescence properties (PL). XRD results indicated that the ZnO nano-columns are free of any impurity phase and crystallize in the hexagonal structure. Typical FT-IR spectra for ZnO nano-columns presented well defined bands, indicating a substantial short-range order in the system. PL spectra consist of a broad band at 590 nm and narrow band at 480 nm corresponding to a near-band edge emission related to the recombination of excitons and level emission related to structural defects. These results show that the HTMW synthesis route is rapid, cost effective, and could be used as an alternative to obtain ZnO nano-columns in the temperature of 120 °C for 8 min.



## 1. Introduction

Order and disorder of the material are the keys to many unsolved structural issues and unexplained structure-related properties in solid materials. In particular, structural order–disorder are always present in real materials and may play an important role in technological applications by altering their electronic and optical properties.

Zinc oxide (ZnO) is an important multifunctional material with applications such as LED's [1,2], gas sensors [3,4], SAW devices [5], solar cells [6,7], catalysts [8,9] and specially as the most promising semiconductor material host, which exhibits ferromagnetism when doped with most of the transition metals including Co, Ni, etc. [10]. The various applications of ZnO are due to specific chemical, surface and microstructural properties of this material [5]. This oxide can form three distinct structures: cubic zinc blende, *rocksalt* and the thermodynamically stable phase zincite, with the wurtzite crystal structure, which can be described as a number of alternating planes composed of tetrahedrally coordinated oxygen anions and zinc cations stacked alternately along the *c*-axis [11]. The rocksalt structure is only observed in relatively high pressures about 10 GPa [12].

Besides the potential applications of ZnO nanostructures in a range of subjects, they also present photoluminescence properties that are useful to investigate structural defects and impurities [13]. The characteristic photoluminescence peaks in the UV band are observed due to direct recombination of electrons in Zn 4p conduction band with holes in O 2p valence band, while the broad visible emission band has been suggested due to the presence of many point defects, such as oxygen vacancies [14,15]. In hydrothermal synthesis the formation of crystal nuclei begins when the concentration of ZnO reaches super saturation, due to the dehydration of $Zn(OH)^{-2}_4$ ions, which acts as the growth unit of ZnO nanostructures [16–18], as a result, the fast growing of ZnO nanostructures lead to smaller surface areas, and the faces whose normal directions correspond to slow growing dominate the final morphology [19–21]. Lima et al. [22] obtained ZnO single crystals, using microwave-hydrothermal method, with reaction times ranging from 15 min to 2 h. Results of the PL emission of ZnO crystalline structures recorded with a 488 nm wavelength argon-ion laser indicated broad

* Corresponding author. Tel.: +55 12 3123 2228; fax: +55 12 3123 2868.
*E-mail address:* alezipo@yahoo.com (A.Z. Simões).
[1] Tel.: +55 12 3123 2228.
[2] Tel.: +55 31 3834 6472/6136; fax: +55 31 3834 6472/6136.
[3] Tel.: +55 16 3301 9828.

0025-5408/$ – see front matter © 2013 Elsevier Ltd. All rights reserved.
http://dx.doi.org/10.1016/j.materresbull.2013.09.049

luminescence behavior in the visible-range spectra. In the case of samples annealed at 2 h, presenting high crystallinity (long-range order), ZnO powders exhibited low emission of the red PL component and blue PL component (498 nm, blue). The powder annealed at 15 min using the conventional hydrothermal method also presented a low blue PL emission. Besides the common use of microwave-hydrothermal method to obtain ZnO, it proved to be effective in the synthesis of other metal oxides, such as CuO, PdO, $Nd_2O_3$, $CeO_2$, gadolinium-doped $CeO_2$ and others, obtained by authors of this group [23–26].

In a conventional heating oven, the heat first reaches the surface of the material. As the heating is kept, the temperature inside the sample gradually increases to equilibrate with the surface, and the equilibrium is reached. In the liquid phase preparation of inorganic nanostructures, most of the synthesis are carried out by conductive heating with an external heat source, like an oil bath, heating mantle or a furnace, which are very slow and rather inefficient, because they depend on convection currents and on the thermal conductivity of the various materials that have to be penetrated, and often the temperature of the reaction vessel is considerably higher than of the reaction mixture. Microwave irradiation, on the other hand, produces efficient internal heating, increasing the temperature of the whole volume simultaneously and uniformly. This technique can provide the following advantages in comparison to conventional heating for chemical synthesis: high heating rates, thus increasing the reaction rates, no direct contact between the heating source and the reactants and/or solvents, excellent control of the reaction parameters, which is not only important with respect to the quality of the product, but also addresses a serious safety issue, selective heating if the reaction mixture contains compounds with different microwave absorbing properties, better selectivity due to reduced side reactions, improved reproducibility, automatized and high throughput synthesis. In addition to these numerous advantages, microwave chemistry also has some significant limitations such as short penetration depth of microwave irradiation into the liquid medium, limiting the size of the reactors, which is a serious problem for scale-up, besides the difficulty to monitor nanostructure formation in situ under reaction conditions [27–35].

de Moura et al. [36] have obtained zinc oxide (ZnO) architectures by an efficient microwave-assisted hydrothermal (MAH) method using a cationic surfactant, cetyltrimethylammonium bromide (CTAB), as the structure-directing template. The ZnO nanostructures were obtained under hydrothermal conditions at 130 °C for 30, 60, 120 and 180 min. Wire-like and flower-like ZnO nanostructures and microstructures were easily prepared using a CTAB structure-directing template MAH method at a short time and a low temperature as compared to the conventional hydrothermal process. PL spectra consist of two bands related to the recombination of excitons and level emission related to structural defects. Macario et al. obtained $BaZrO_3$ microcrystals using the microwave assisted hydrothermal method at 140 °C for 40 min. The authors have obtained nanostructures free of impurities at lower temperature and reaction time, proving its efficacy [37].

The present work focuses on the photoluminescent behavior of ZnO nano-columns, investigating the role of MAH and the mineralizer agent (KOH) on the PL emission in the absence of CTAB (a cationic surfactant), which decreases the energy needed to form ZnO phase. This research involves four critical steps: (1) synthesis of the nano-columns; (2) structural characterization; (3) establishing the purity of the ZnO phase; and more importantly, (4) revealing the relationship between structural defects and the PL properties at lower soaking time compared with previous results obtained via hydrothermal microwave method.

## 2. Experimental procedure

Zinc acetate dihydrate ($(CH_3CO_2)_2Zn{\cdot}2H_2O$) was dissolved in a solution of ethyl alcohol and acetylacetone ($CH_3COCH_2COCH_3$) at 60 °C for 1 h. ZnO nano-columns were synthesized by a hydrothermal microwave route. Zinc acetate dihydrate ($5 \times 10^{-3}$ mol $L^{-1}$, 99.9% purity) was dissolved in 80 ml of deionized water under constant stirring for 15 min at room temperature. Subsequently, 2 M KOH (p.a, Merck) was slowly added in the solution until the pH 10. The resulting solution was transferred into a sealed Teflon autoclave and placed in a hydrothermal microwave (2.45 GHz, maximum power of 800 W). The reactional system was heat treated at 120 °C for 8 min with a heating rate fixed at 10 °C/min. The pressure in the sealed autoclave was stabilized at 1.2 atm. The autoclave was cooled to room temperature naturally. ZnO nano-columns were collected and washed with acetone several times and then dried at 80 °C in an oven until pH 7.

Thermal effect was investigated by thermogravimetric analysis (TGA) and differential thermal analysis (DTA) in the apparatus STA 409, Netzsch, Germany. Synthetic air flow (30 $cm^3$/min) with a constant heating rate of 5 °C/min from room temperature up to 1200 °C was used. The obtained nano-columns were characterized by X-ray powder diffraction (XRD) using a (Rigaku-DMax/2500PC, Japan) with Cu-Kα radiation (λ = 1.5406 Å) in the 2$\theta$ range from 20 to 80° with 0.2°/min. The crystallite size ($d$) of ZnO was calculated using Scherrer equation $d = k\lambda/\beta \cos\theta$, where $k$ is constant, λ is wavelength of X-rays and $\beta$ is the full width at half maximum (FWHM) for (1 1 1) reflection measured from slow scan where $\theta$ is the diffraction angle of the main peak. A 1064 nm YAG laser was used as the excitation source, and its power was kept at 150 mW. The FT-IR spectra were recorded with a Bruker Equinox-55 instrument. Infrared spectroscopy was used for monitoring the structural changes occurring during the synthesis process with the KBr pellet technique. The morphology of as-prepared samples was observed using a high resolution field-emission gun scanning electron microscopy FEG-SEM (Supra 35-VP, Carl Zeiss, Germany). Specimens for TEM were obtained by drying droplets of as-prepared samples from an ethanolic dispersion which had been sonicated for 5 min onto 300 mesh Cu grids. TEM, HRTEM images and SAD patterns were then taken at an accelerating voltage of 200 kV on a Philips model CM 200 instrument. PL properties were measured with a Thermal Jarrel-Ash Monospec27 monochromator and a Hamamatsu R446 photomultiplier. The excitation source was 350.7 nm wavelength of a krypton ion laser (Coherent Innova), keeping their power at 200 mW. All measurements were performed at room temperature.

## 3. Results and discussion

### 3.1. Thermal analyses

Having in mind that ZnO powder obtained at 120 °C for 8 min contains slight traces of impurity, we have performed TG-DTA analyses (Fig. 1). TG/DTA curves of the ($(CH_3CO_2)_2Zn{\cdot}2H_2O$) precursor solution obtained from room temperature up to 1200 °C using a heating rate of 5 °C/min is shown in Fig. 1. The existence of three stages corresponding to the weight and energy change can be observed. The first region (25–200 °C) corresponds to the loss of physisorbed water; the second between 200 and 350 °C corresponds to the loss of surface hydroxyl groups, and finally, the weight loss above 500 °C is due to $CO_2$ released from the decomposition of carbonate species. DTA curve shows a strong exothermic peak around 270–350 °C, correlated to a weight loss that must be considered as the crystallization of the residual

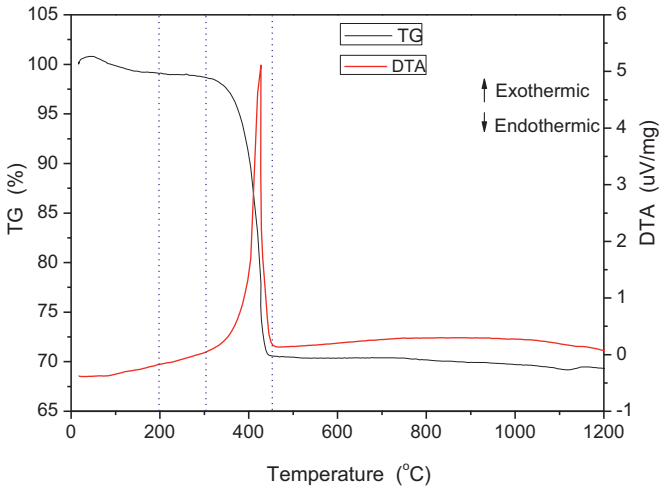


**Fig. 1.** TG/DTA curves of the ZnO precursor annealed from room temperature to 1200 °C.

amorphous phase [19]. It should be noticed that above 450 °C the ZnO stable phase was formed.

### 3.2. X-ray diffraction analyses

Fig. 2 shows the XRD diffraction pattern of the ZnO nano-columns. The diffraction peaks in the pattern can be indexed to hexagonal wurtzite structured ZnO (space group: P63mc (186); $a = 0.3249$ nm, $c = 0.5206$ nm) and diffraction results are in agreement with JCPDS card for ZnO (JCPDS 036-1451) [34]. The intensity of the peaks relative to the background signal demonstrates hexagonal phase of the products and high crystallinity of the ZnO phase. The characteristic peaks of $Zn(OH)_2$ were not observed, which indicated a single phase hexagonal ZnO. The nanocrystallites are oriented along the *c*-axis, [1 0 1] direction. The narrow peaks indicate good sample crystallinity, demonstrating that ZnO nano-columns obtained after 8 min using MAH process present a long-range periodicity. The mean grain size ($d$) of the ZnO nanostructured samples was calculated using Scherrer's equation. The average grain size determined from XRD pattern was 3.9 nm.

### 3.3. FT-IR analyses

Fig. 3 shows FTIR spectral features of ZnO nano-columns. Strong intense bands at 3448, 2358, 1589, 1075 $cm^{-1}$ and below 700 $cm^{-1}$ were observed. The bands at 3435 and 1589 $cm^{-1}$ correspond to the $\nu$ (O–H) mode of (H-bonded) water molecules and $\delta$ (OH), respectively. Residual water and hydroxy group are usually detected in the as prepared samples regardless of synthesis method used [35] and further heat treatment is necessary for their elimination. It is well known that the hydroxylation of metal ions and the deprotonation can be accelerated by raising the solution temperature or pressure. In hydrothermal-microwave processing the high frequency electromagnetic radiation interacts with the permanent dipole of the liquid ($H_2O$), which initiates rapid heating from the resultant molecular rotation. Likewise, permanent or induced dipoles in the dispersed phase cause rapid heating of the particles. These result in a reaction temperature in excess of the surrounding liquid-localized superheating [36]. The FT-IR spectrum also exhibits strong broad band below 700 $cm^{-1}$ which is due to the $\delta$ (Zn–O–Zn) mode. Specifically, the strong absorptive peaks at 400–600 $cm^{-1}$ were attribute to the Zn–O stretching and bending vibration, being characteristics of the tetrahedral $ZnO_4$ groups in the compounds.

### 3.4. FEG-SEM analyses

FEG-SEM micrographs of ZnO nano-column obtained at different magnifications are shown in Fig. 4. The synthesis process by the MAH method accelerates the ZnO crystallization which leads to the formation of material at a low temperature and a short reaction time. Weakly aggregation between the particles is observed indicating that $Zn(OH)_x$ was transformed to ZnO after hydrothermal treatment and Van der Waal's force is reduced. Moreover, the distribution in size seemed to be homogeneous and the shape consists of ZnO multiwires with a flower-like shape of about 50–400 nm in width and several micrometers in length have a clean surface and present a hexagonal cross-section with a six-fold pyramidal geometry in the extremity. In the hydrothermal process, the presence of an alkaline medium was found to be essential. During the hydrothermal treatment, $Zn^{+4}$ hydroxides underwent an attack by basic medium to dissolve and react at high temperatures and pressures, and then precipitated as insoluble

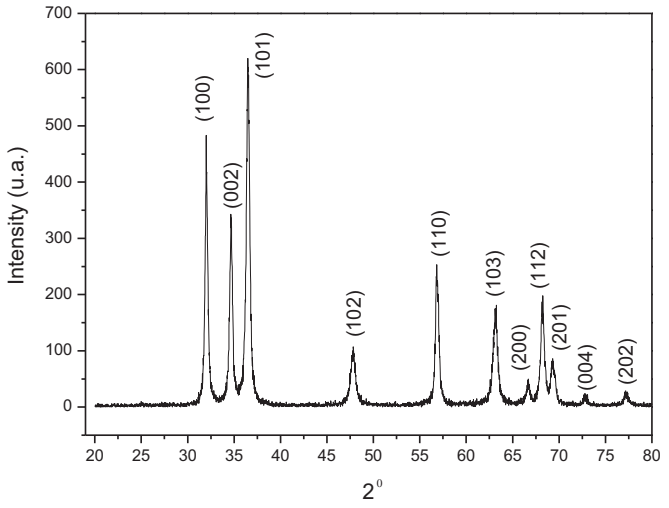


**Fig. 2.** XRD pattern of the ZnO nano-columns obtained in the hydrothermal microwave method at 120 °C for 8 min.

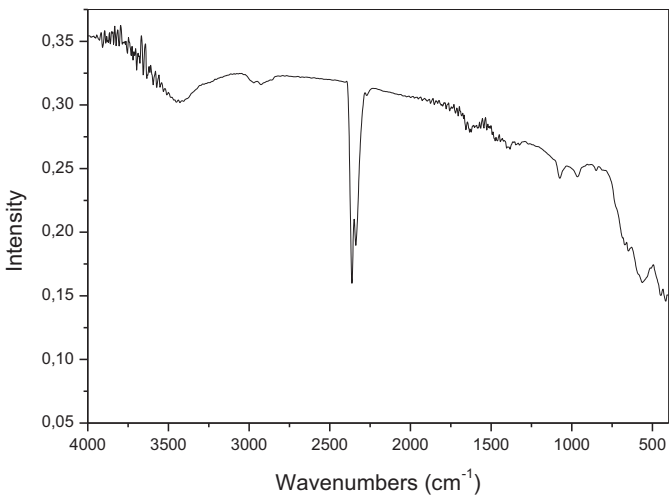


**Fig. 3.** FT-IR pattern of the ZnO nano-columns obtained in the hydrothermal microwave method at 120 °C for 8 min.

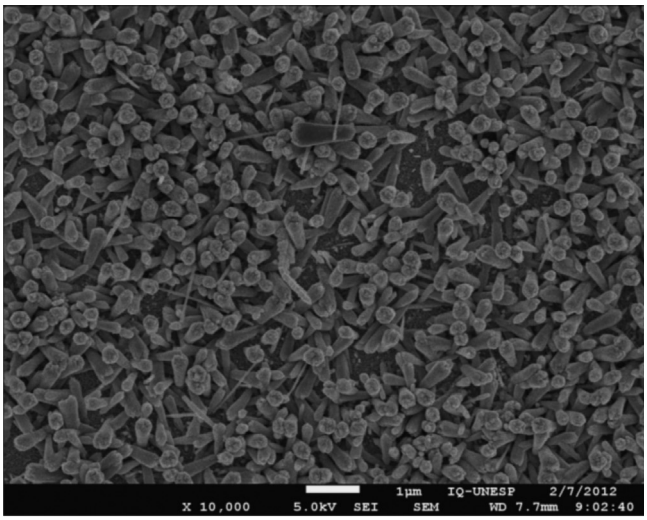


(a)

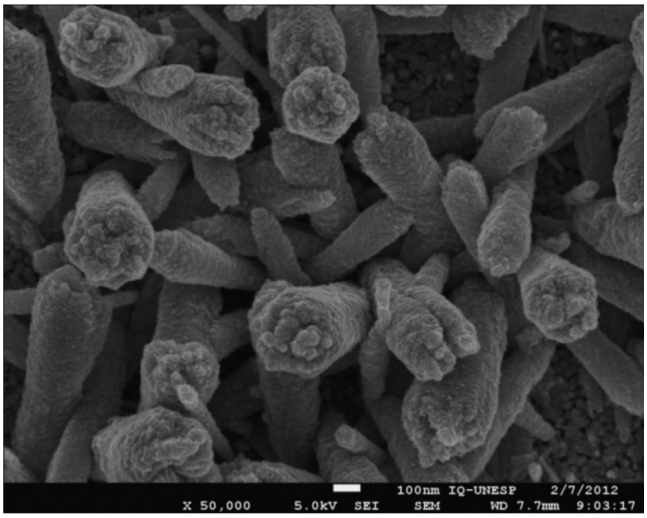


(b)

**Fig. 4.** FEG-SEM of the ZnO nano-columns obtained in the hydrothermal microwave method at 120 °C for 8 min showing: (a) 1 μm and (b) 100 nm.

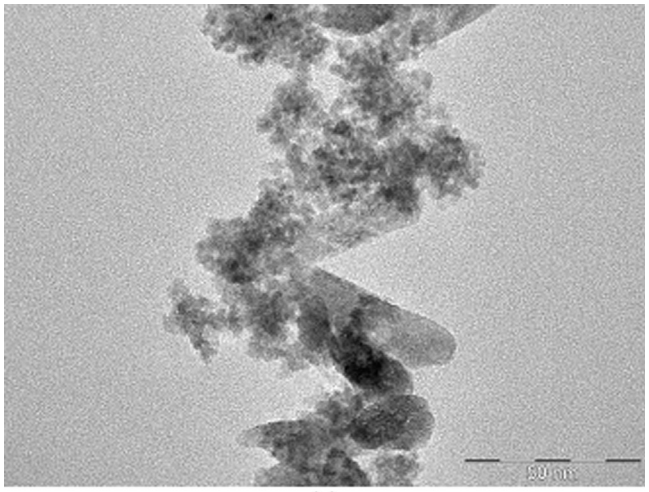

(a)

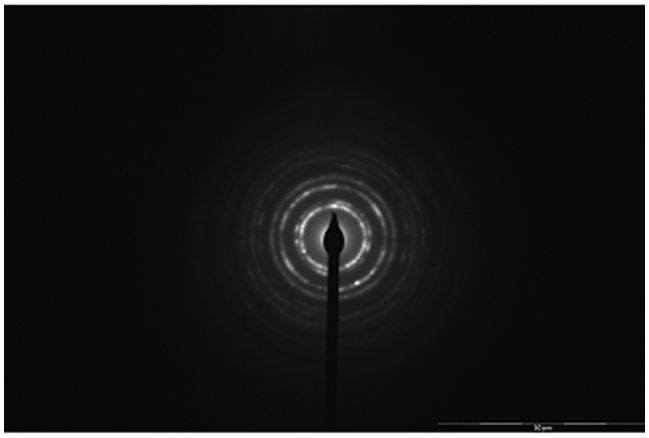

(b)

**Fig. 5.** (a) TEM of the ZnO nano-columns obtained in the hydrothermal microwave method at 120 °C for 8 min and (b) SAD of the ZnO nano-columns obtained in the hydrothermal microwave method at 120 °C for 8 min.

ceramic oxide particles from the supersaturated hydrothermal fluid. If the temperature and pressure conditions are carefully maintained during the duration of the experiment, neither etching of ZnO crystals nor the formation of agglomerates is observed. Therefore, the dissolution and crystallization process continued in supersaturated fluid in such a way that the system was self-stabilizing. The ZnO consists of non-stoichiometric ZnO, which contains bulk oxygen vacancies and interstitial oxygen ions that act as donor states. These states permit the adsorption of oxygen. When oxygen molecule gets adsorbed at the ZnO nano-column surface or at the grain boundaries, it extracts electrons from the conduction band, thus, reducing the concentration of the electrons. As adsorbed oxygen concentration increases, the number of conduction band electrons decreases further and the ZnO nano-column becomes more resistive.

### 3.5. TEM analyses

The typical flower-like ZnO architectures composed of multiple ZnO wires as swords or pointed wires are observed in Fig. 5a as shown in the TEM image. Fig. 5b shows the selected area electron diffraction (SAD) pattern indicating a single crystalline character of the nanowires and microwires indexed as the hexagonal ZnO phase which is in agreement with XRD presented in Fig. 2. ZnO crystallizes in a hexagonal wurtzite structure (space group: *P*63*mc* (186); $a = 3.242$ Å, $c = 5.196$ Å), according to JCPDS card 36-1451. The high purity of the ZnO hexagonal phase and good crystallinity, demonstrating that ZnO nano-columns obtained by hydrothermal conditions present a long range order or periodicity (completely ordered structure) being the lattice parameters values quite similar to the XRD analyses. SAD indicates that the growth direction of wires is [1 0 1]. The facets forming these nanowires and microwires can be polar and nonpolar and new theoretical analysis of the corresponding values of the surface energy of both polar and nonpolar facets of the ZnO system is being calculated. These results imply that the *c*-axis ((1 0 1) direction) is the fast growth direction for ZnO structures. The particles do not grow beyond such magnitude because it is postulated that at the start of the reaction a large number of nucleus forms in the solution and as the reaction takes place in a very dilute solution there is not enough reactant left for the growth of the particles. The MAH process at KOH mineralizer showed efficiency to dehydrate the adsorbed water and decrease the hydrogen bonding effect leaving a weakly agglomerated nano-column of hydrated zinc. Alternatively, if the solution was maintained at basicity, it might be due to

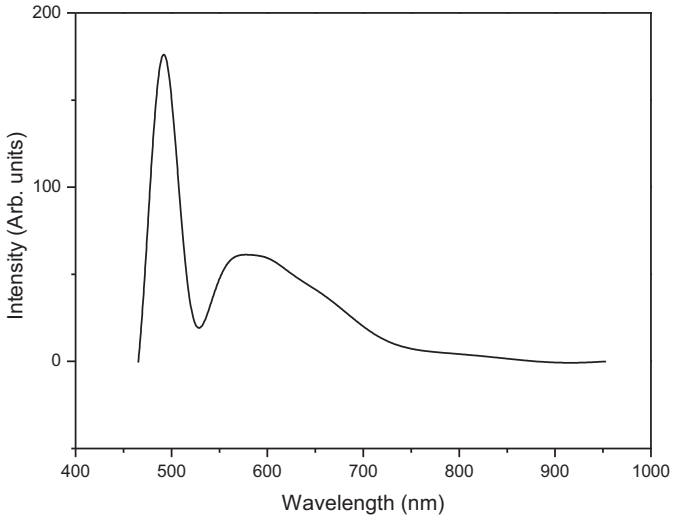


**Fig. 6.** PL spectra at room temperature of the ZnO nano-columns obtained in the hydrothermal microwave method at 120 °C for 8 min.

crystallization from amorphous gel through a dissolution–precipitation, because solubility of zinc hydroxide is very high in the strong basic solution. This behavior indicates that ZnO nano-columns showed a fewer amount of water on the particles surfaces, so that hydrogen bonds cannot be formed between approaching particles. In the microwave heating process, the introduction of electromagnetic microwave radiation offers significant advantages over the conventional heating method. Furthermore, rapid heating under hydrothermal conditions of pressure and temperature offers higher mobility of dissolved ions and molecules and accelerates solid particles to high velocities, increasing the collision rate and effective fusion at the collision point [36,16]. Microwave heating led to the formation of crystalline fine particles with a homogeneous distribution at low temperatures and short treatment times.

### 3.6. Photoluminescence properties

Fig. 6 shows the PL spectra of ZnO nano-columns synthesized by MAH under KOH at 120 °C for 8 min. ZnO nano-columns with polycrystalline characteristic present two peaks: at 490 nm (blue-green emission) and the other at 580 nm (green emission). Intense and broad PL with a maximum at around 490 nm in the visible region (orange) is noted. This intensity is likely associated with the structure organization level [38], and the charge transfer occurring between oxygen and zinc ions. The characteristic photoluminescence peaks in the UV band are observed due to direct recombination of electrons in Zn 4p conduction band with holes in O 2p valence band, while the broad visible emission band has been suggested due to the presence of many point defects, such as oxygen vacancies. In the hydrothermal synthesis of ZnO, the formation of crystal nuclei of its nanostructures begins when the concentration of ZnO reaches supersaturation, and generally, the faces perpendicular to the fast direction of growth have smaller surface areas and the faces whose normal directions correspond to slow growing ones thus dominate the final morphology.

## 4. Conclusions

Adopting the microwave–hydrothermal process as synthesis method it is possible to obtain, by treating the solution at 120 °C for only 8 min, nanometric and crystalline zinc oxide nano-columns. The hydrothermal reaction to grow ZnO crystallites with a pure phase can be described by the dissolution–crystallization process. FEG-SEM analyses have shown a homogeneous size distribution of nanometric ZnO crystallites under KOH mineralizer agent. This can be explained by the low amount of hydrogen bonds during the drying and calcining process. TEM image shows typical flower-like ZnO architectures composed of multiple ZnO wires as swords or pointed wires. PL emission reveals two peaks which can be understood as the direct recombination of electrons in Zn 4p conduction band with holes in O 2p valence band and the presence of various point defects (oxygen vacancies) in the ZnO lattice. MAH is important not only for the use of a short treatment time and low temperature but also for the possibility to control the morphological and structural properties. Therefore, the MAH method is undeniably a genuine technique for low temperatures and short times in comparison with the previous methodologies.

## Acknowledgments

The financial support of this research project by the Brazilian research funding agencies CNPq and FAPESP is gratefully acknowledged. We also gratefully acknowledged Professor José Arana Varela and Diogo Volanti for TEM facilities.

## References

[1] O. Singh, M.P. Singh, N. Kohli, R.C. Singh, Effect of pH on the morphology and gas sensing properties of ZnO nanostructures, Sens. Actuators B 166 (2012) 438.
[2] D.C. Kim, W.S. Han, B.H. Kong, H.K. Cho, C.H. Hong, Fabrication of the hybrid ZnO LED structure grown on p-type GaN by metal organic chemical vapor deposition, Physica B 401 (2007) 386.
[3] Y. Zhou, D. Li, X. Zhang, J. Chen, S. Zhang, Facile synthesis of ZnO micro-nanostructures with controllable morphology and their applications in dye-sensitized solar cells, Appl. Surf. Sci. 261 (2012) 759.
[4] J. Yi, J.M. Lee, W.I. Park, Vertically aligned ZnO nanorods and graphene hybrid architectures for high-sensitive flexible gas sensors, Sens. Actuators B: Chem. 115 (2011) 264.
[5] S. Roy, S. Basu, Improved zinc oxide film for gas sensor applications, Bull. Mater. Sci. 25 (2002) 513.
[6] X. Xu, M. Wu, M. Asoro, P.J. Ferreira, D.L. Fan, One-step hydrothermal synthesis of comb-like ZnO nanostructures, Cryst. Growth Des. 12 (2012) 4829.
[7] S.M. Mahpeykar, J. Koohsorkhi, H. Ghafoori-fard, Ultra-fast microwave-assisted hydrothermal synthesis of long vertically aligned ZnO nanowires for dye-sensitized solar cell application, Nanotechnology 23 (2012) 165602.
[8] S.A. Khayyat, M.S. Akhtar, A. Umar, ZnO nanocapsules for photocatalytic degradation of thionine, Mater. Lett. 81 (2012) 239.
[9] A. Kajbafvala, H. Ghorbani, A. Paravar, J.P. Samberg, E. Kajbafvala, S.K. Sadrnezhaad, Effects of morphology on photocatalytic performance of zinc oxide nanostructures synthesized by rapid microwave irradiation methods, Superlattices Microstruct. 51 (2012) 512.
[10] B. Hadzic, N. Romcevic, M. Romcevic, I.K. Kudelska, W. Dobrowolski, J. Trajic, D. Timotijevic, U. Narkiewicz, D. Sibera, Surface optical phonons in ZnO(Co) nanocolumns: Raman study, J. Alloys Compd. 540 (2012) 49.
[11] R.C. Pawar, J.S. Shaikh, S.S. Suryavanshi, P.S. Patil, Growth of ZnO nanodisk, nanospindles and nanoflowers for gas sensor: pH dependency, Curr. Appl. Phys. 12 (2012) 778.
[12] P.R. Sajanlal, T.S. Sreeprasad, A.K. Samal, T. Pradeep, Anisotropic nanomaterials: structure, growth, assembly, and functions, Nano Rev. 2 (2011) 1.
[13] Z. Zhu, D. Yang, H. Liu, Microwave-assisted hydrothermal synthesis of ZnO rod-assembled microspheres and their photocatalytic performances, Adv. Powder Technol. 22 (2011) 493.
[14] S.K. Gupta, A. Joshi, M. Kaur, Development of gas sensors using ZnO nanostructures, J. Chem. Sci. 122 (2010) 57.
[15] S. Boudjadar, S. Achour, N. Boukhenoufa, L. Guerbous, Microwave hydrothermal synthesis and characterization of ZnO nanosheets, Int. J. Nanosci. 9 (2010) 585.
[16] J. Huang, C. Xia, L. Cao, X. Zeng, Facile microwave hydrothermal synthesis of zinc oxide one-dimensional nanostructure with three-dimensional morphology, Mater. Sci. Eng. B 150 (2008) 187.
[17] W.J. Li, E.W. Shi, W.Z. Zhong, Z.W. Yin, Growth mechanism and growth habit of oxide crystals, J. Cryst. Growth 203 (1999) 186.
[18] S. Yamabi, H. Imai, Growth conditions for wurtzite zinc oxide films in aqueous solutions, J. Mater. Chem. 12 (2002) 3773.
[19] C. Li, X. Du, W. Lu, K. Liu, J. Chang, S. Chen, D. Yue, Z. Wang, Luminescent single-crystal ZnO nanorods: controlled synthesis through altering the solvents composition, Mater. Lett. 81 (2012) 229.
[20] Q. Jiang, Y. Liu, H. Kan, B. Yuan, H. Zhao, Microwave-assisted synthesis of hexagonal structure ZnO micro-tubes, Mater. Lett. 81 (2012) 198.
[21] M. Baghbanzadeh, S.D. Skapin, Z.C. Orel, C.O. Kappe, A critical assessment of the specific role of microwave irradiation in the synthesis of ZnO micro- and nanostructured materials, Chemistry 18 (2012) 5724.

[22] R.C. Lima, L.R. Macario, J.W.M. Espinosa, V.M. Longo, R. Erlo, N.L. Marana, J.R. Sambrano, M.L. dos Santos, A.P. Moura, P.S. Pizani, J. Andrés, E. Longo, J.A. Varela, Toward and understanding of intermediate and short-range defects in ZnO single crystals: a combined experimental and theoretical study, J. Phys. Chem. A 112 (2008) 8970.
[23] D.P. Volanti, M.O. Orlandi, J. Andrés, E. Longo, Efficient microwave-assisted hydrothermal synthesis of CuO sea urchin-like architectures *via* a mesoscale self-assembly, Cryst. Eng. Commun. 12 (2010) 1696.
[24] I. Bilecka, M. Niederberger, Microwave chemistry for inorganic nanomaterials synthesis, Nanoscale 2 (2012) 1358.
[25] Y. Shen, L. Li, Q. Lu, J. Ji, R. Fei, J. Zhang, E.S. Abdel-Halim, J.J. Zhu, Microwave-assisted synthesis of highly luminescent CdSeTe@ZnS–$SiO_2$ quantum dots and their application in the detection of Cu(II), Chem. Commun. 48 (2012) 2222.
[26] A.L. Washington I.I., G.F. Strouse, Microwave synthesis of CdSe and CdTe nanocrystals in nonabsorbing alkanes, J. Am. Chem. Soc. 130 (2008) 8916.
[27] P. Chand, A. Gaur, A. Kumar, Structural and optical properties of ZnO nanocolumns synthesized at different pH values, J. Alloys Compd. 539 (2012) 174.
[28] S.S. Alias, A.B. Ismail, A.A. Mohamad, Effect of pH on ZnO nanoparticle properties synthesized by sol–gel centrifugation, J. Alloys Compd. 499 (2010) 231.
[29] A. Stankovic, Z. Stojanovic, L. Veselinovic, S.D. Skapin, I. Bracko, S. Markovic, D. Uskokovic, ZnO micro and nanocrystals with enhanced visible light absorption, Mater. Sci. Eng. B 177 (2012) 1038.
[30] A. Outzourhit, Characterization of hydrothermally prepared $BaTi_{1-x}Zr_xO_3$, J. Alloys Compd. 340 (2002) 214.
[31] Q. Roy, H. Li, Microwave-hydrothermal synthesis of ceramic powders, Mater. Res. Bull. 27 (1992) 1393.
[32] S. Komarneni, Q.H. Li, R. Roy, Microwave-hydrothermal processing of layered anion exchangers, J. Mater. Res. 11 (1996) 1866.
[33] A.P. de Moura, R.C. Lima, M.L. Moreira, D.P. Volanti, J.W.M. Espinosa, M.O. Orlandi, P.S. Pizani, J.A. Varela, E. Longo, ZnO architectures synthesized by a microwave-assisted hydrothermal method and their photoluminescence properties, Solid State Ionics 181 (2010) 775.
[34] P. Mitra, A.P. Chatterjee, H.S. Maiti, ZnO thin film sensor, Mater. Lett. 35 (1998) 33.
[35] H. Wang, J.J. Zhu, J.M. Zhu, S. Xu, T. Ding, Preparation of nanocrystalline ceria particles by sonochemical and microwave assisted heating methods, Phys. Chem. 4 (2002) 3794.
[36] M.L. Moreira, G.P. Mambrini, D.P. Volanti, E.R. Leite, M.O. Orlandi, P.S. Pizani, V.R. Mastelaro, C.O. Paiva-Santos, E. Longo, J.A. Varela, Hydrothermal microwave: a new route to obtain photoluminescent crystalline $BaTiO_3$ nano-columns, Chem. Mater. 20 (2008) 5381.
[37] L.R. Macario, L. Mario, Moreira, Juan Andrés, Elson Longo, An efficient microwave-assisted hydrothermal synthesis of $BaZrO_3$ microcrystals: growth mechanism and photoluminescence emissions, Chem. Eng. Commun. 12 (2010) 3612.
[38] C. Liu, H. Li, W.J.X. Zhang, D. Yu, ZnO architectures synthesized by a microwave-assisted hydrothermal method and their photoluminescence properties, Mater. Lett. 60 (2006) 1394.